UNIFORMED SERVICES UNIVERSITY OF THE HEALTH SCIENCES
4301 JONES BRIDGE ROAD
BETHESDA, MARYLAND 20814-4799

06 JULY 2004

APPROVAL SHEET

Title of Thesis: "Comparison of Experimental Models for Predicting Laser Tissue Interaction from 3.8-Micron Lasers"

Name of Candidate: 1Lt Piper C.M. Williams
Master of Science in Public Health
Department of Preventive Medicine and Biometrics

Thesis and Abstract Approval:

_____	_____
Chairman: Maj Scott A. Nemmers, PhD.	Date
_____	_____
Research Advisor: Thomas E. Johnson, PhD.	Date
_____	_____
CDR Gary L. Hook, Ph.D.	Date
_____	_____
Lt Col Peter T. LaPuma, PhD.	Date
_____	_____
LTC (Dr) Michael J. Roy	Date

Report Documentation Page

Form Approved
OMB No. 0704-0188

1. REPORT DATE	2. REPORT TYPE	3. DATES COVERED
2004		**-**

4. TITLE AND SUBTITLE	5a. CONTRACT NUMBER
Comparison of Experimental Models for Predicting Laser Tissue Interaction from 3.8-Micron Lasers	5b. GRANT NUMBER
	5c. PROGRAM ELEMENT NUMBER
6. AUTHOR(S)	5d. PROJECT NUMBER
	5e. TASK NUMBER
	5f. WORK UNIT NUMBER
7. PERFORMING ORGANIZATION NAME(S) AND ADDRESS(ES) **Uniformed Servicces universsity of the Health Sciences,F. Edward Herbert School of Medicine,4301 Jones Bridge Road,Bethesda,MD,20814-4799**	8. PERFORMING ORGANIZATION REPORT NUMBER
9. SPONSORING/MONITORING AGENCY NAME(S) AND ADDRESS(ES)	10. SPONSOR/MONITOR'S ACRONYM(S)
	11. SPONSOR/MONITOR'S REPORT NUMBER(S)

12. DISTRIBUTION/AVAILABILITY STATEMENT
Approved for public release; distribution unlimited

13. SUPPLEMENTARY NOTES
The original document contains color images.

14. ABSTRACT

The purpose of this study was to compare and contrast the effects of single 3.8-micron laser pulses in an in-vitro and in-vivo model of human skin and to demonstrate the efficacy of in-vitro laser tissue interaction models. The minimum exposure required to produce specific, gross morphologic changes from a four microsecond, pulsed skin exposure for both models was determined. Histologic samples of the tissues were compared to ascertain the effectiveness of the in-vitro models. Eighteen artificial skin equivalents, (in-vitro model), were exposed and compared to exposures made on five Yorkshire pigs. Representative biopsies were taken for histologic evaluation from various locations immediately, one hour, and 24 hours following exposure. The pattern of epithelial changes seen following in-vivo exposure of pig skin was similar to the changes previously observed in human skin equivalents, indicating that the artificial skin equivalents are representative in-vitro models for this particular combination of laser parameters.

15. SUBJECT TERMS

16. SECURITY CLASSIFICATION OF:			17. LIMITATION OF ABSTRACT	18. NUMBER OF PAGES	19a. NAME OF RESPONSIBLE PERSON
a. REPORT	b. ABSTRACT	c. THIS PAGE			
unclassified	**unclassified**	**unclassified**		**44**	

The author hereby certifies that the use of any copyrighted material in the thesis manuscript entitled:

"Comparison of Experimental Models for Predicting Laser Tissue Interaction from 3.8-micron Lasers"

beyond brief excerpts is with the permission of the copyright owner, and will save and hold harmless the Uniformed Services University of the Health Sciences from any damage, which may arise from such copyright violations.

Piper C.M. Williams
1Lt, USAF, BSC
Department of Preventive Medicine and Biometrics
Uniformed Services University of the Health Sciences

ABSTRACT

Title of Thesis: "Comparison of Experimental Models for Predicting Laser Tissue Interaction from 3.8-Micron Lasers"

Author: 1Lt Piper C.M. Williams

Master of Science in Public Health

Thesis Directed by: Thomas E. Johnson

Assistant Professor

Department of Preventive Medicine and Biometrics

The purpose of this study was to compare and contrast the effects of single 3.8-micron laser pulses in an *in-vitro* and *in-vivo* model of human skin and to demonstrate the efficacy of *in-vitro* laser tissue interaction models. The minimum exposure required to produce specific, gross morphologic changes from a four microsecond, pulsed skin exposure for both models was determined. Histologic samples of the tissues were compared to ascertain the effectiveness of the *in-vitro* models. Eighteen artificial skin equivalents, (*in-vitro* model), were exposed and compared to exposures made on five Yorkshire pigs. Representative biopsies were taken for histologic evaluation from various locations immediately, one hour, and 24 hours following exposure. The pattern of epithelial changes seen following *in-vivo* exposure of pig skin was similar to the changes previously observed in human skin equivalents, indicating that the artificial skin equivalents are representative *in-vitro* models for this particular combination of laser parameters.

Comparison of Experimental Models for Predicting Laser Tissue Interaction from 3.8-Micron Lasers

BY

1LT PIPER C.M. WILLIAMS

Thesis submitted to the Faculty of the Department of Preventive Medicine and Biometrics and the Department of Radiology/Radiological Sciences Graduate Program of the Uniformed Services University of the Health Sciences in partial fulfillment of the requirements for the Degree of Master of Sciences in Public Health, 2004

ACKNOWLEDGMENT

A great big thank you goes to the talented PMB laser team, Don Q. Randolph, Golda C.H. Winston, and Laticia Saunders for their patience and help anytime I needed a hand. I would also like to thank Sue Pletcher for preparing and re-preparing countless slides. Thank you to Dr. Thomas Eurell whose human skin equivalents and expertise made this study possible.

I would like to thank all the members of my committee for their time and assistance in helping complete this program. Very special thanks goes to Major Scott Nemmers for keeping me calm even at my most distraught moments and Dr. Thomas E. Johnson for inspiring me with his unfailing optimism.

DEDICATION

To P.B. for your unconditional patience and support through all the victories and defeats. To my wonderfully loving parents, Michele and Ted Williams, I thank you for believing in me even when I did not believe in myself. To my brother Blue, for inspiring me to live outside the box. And of course, to the incomparable D.T.D. I dedicate this thesis to all of you.

TABLE OF CONTENTS

LIST OF FIGURES

LIST OF TABLES

LIST OF GRAPHS

CHAPTER ONE: INTRODUCTION

Background and Significance

Little information is available on the skin effects of laser systems operating in the 3.8-micron region. With the exception of the medical free-electron laser, (MFEL) it is an untested, seldom used wavelength (Edwards et al.**)**. At this time there is little scientific evidence to support the current American National Standard Institute's, (ANSI Z136. 1-2000), maximum permissible exposure (MPE) value, for skin at this wavelength. The current skin MPE value serves to prevent thermal injury (ANSI Z136. 1-2000). An MPE is chosen below known hazardous exposure levels based on the best available information. However, due to a lack of research at this wavelength, the MPE value for skin appears to have been extrapolated from studies involving corneal rather than dermal exposure (ANSI Z136. 1-2000**)**. Generally, damage to the eye is considered more serious than damage to the skin because skin damage can be more easily repaired and the long-term effects may not be as dramatic (Steele). Even so, it is imperative to learn more about the thresholds for dermal injury at this wavelength in order to facilitate the improvement of appropriate safety standards.

Two models were chosen to characterize skin responses when exposed to a 3.8-micron laser, the *in-vitro* model (engineered human skin) and *in-vivo* (porcine skin). This baseline comparison can be used to predict skin response in human skin.

Engineered human skin equivalents are anatomically similar to human skin (Whitton and Everall, 1973). They can be grown to include both the dermal and epidermal layers,

including the stratum corneum, stratum granulosum, stratum spinosum, and the stratum basale, (basal layer).

Previous studies have used porcine skin as a surrogate for human skin (Rico et al.; Eggleston et al.). Most studies involving laser insult to skin utilize the Yorkshire pig flank, as opposed to other body areas, more as a matter of convenience than necessarily because of its comparability to human skin (Eggleston et al). Nevertheless, direct comparisons have identified a high degree of similarity between the skin of the Yorkshire porcine flank and that of the human face arms and neck, though the former is not as thick (Meyer et al.; Montagna and Yun).

A better understanding of the laser-tissue interactions for both the engineered human skin, (*in-vitro*) and porcine, (*in-vivo*) models at the 3.8-micron wavelength will make it possible to demarcate each model's most effective and efficient uses, and perhaps even leading to fewer situations of necessary *in-vivo* testing.

Research Objective

The goal of this research is to compare the laser-tissue interactions of the *in-vitro*, human skin equivalent model with the *in-vivo*, porcine skin model, while determining the maximum energy of 3.8-micron single laser pulses that can be safely used without eliciting a response. To accomplish this comparison the following items were examined:

1. The gross presentation of the tissues, both human skin equivalents and porcine skin, after a single four microsecond, pulsed exposure
2. The gross histopathology of biopsies taken from representative exposure sites of both

the human skin equivalents and the porcine skin, and

3. The depth of energy penetration of both the human skin equivalents and the pig skin at representative sites.

CHAPTER TWO: LITERATURE REVIEW

Replacement Modeling

For many years researchers have sought to utilize *in-vitro* models for laser safety and other safety studies. Recent advances in these models prompted the comparison between a new *in-vitro* model with more established *in-vivo* model. There are many advantages to using the *in-vitro* model.

Reducing the number of animals utilized in a study and replacing them with human skin equivalents lends itself to a more efficient research process. For example, less resources are required to procure and maintain the human skin equivalents compared to the animal model. Regulatory authorities require more complex protocols when dealing with animal models (Ponec). Using human cell lines for research makes it unnecessary to have to extrapolate to human responses from animal-derived data. Also, the uniformity of the human skin equivalents makes it easier to reproduce research results. Skin models are being used in many areas of research today including cancer research, the study of the infection processes of specific organisms, as well as, burn, toxicity and irritancy research. To date, there has been limited research in using these models for laser tissue interaction (Eurell et al.).

There are a few varieties of engineered human skin equivalents. There are those equivalents that are made from naturally occurring tissues, like cutaneous allografts (cadaver skin), which have been around since the mid-19th century (Pruitt). Some more modern equivalents are made from synthetic materials, such as a solid silicone polymers and nylon (Pruitt). There are also those created from collagen-based dermal analogs, like

Alloderm and those, as seen in this study, made from culture-derived tissues, like fibroblast or epithelial seeded dermal analogs (Pruitt).

Erythema and Edema

Two common gross reactions seen in skin are erythema and edema. Edema is a result of tissues swelling with fluid. Trauma leads to vasodilatation and increased vascular permeability. Plasma escapes from the vasodilated vessels, into the tissue causing it to distend. When peripheral capillary beds become swollen in congestion, the red blood cells expand. Because there are so many more red than white blood cells, one can see the red through the skin, which is erythema (James et al.). It is important to note that erythema is not a potential reaction with the *in-vitro* model due to its non-vascular nature.

Effective Dose, (ED_{50})

Effective dose, (ED_{50}) is defined as "the dose of a particular substance that elicits an observable response in 50 percent of the test subjects" (James et al.). This research intends to outline each level of observable reaction and calculate its corresponding effective dose, specifically, the fluence necessary to elicit the observed response in 50 percent of the exposed sites.

The ED_{50} is not directly incorporated into safety standards. Instead, a safety factor of ten is typically applied and that value is assigned as the maximum permissible

exposure (James et al.). The current ANSI MPE for cornea and skin is 2.24×10^{-2} J/cm^2 for lasers operating at 3.8-microns for 4-microseconds (ANSI Z136. 1-2000). The ED_{50} on Yorkshire pig skin has been shown to be 43.1 J/cm^2 when exposed to 1540 nm (Roach and Johnson). At 10.6-microns the ED_{50} is 2.8 J/cm^2 (Rockwell et al., 1974). But, research characterizing skin exposures to 3.8-micron lasers are unavailable. Although, it has been shown that *in-vivo* corneas exposed to 3.72-micron laser light for a duration of 0.125 seconds have an ED_{50} of 0.377 J/cm^2 (Dunsky and Egbert); corneas are not skin.

It is difficult to estimate the skin ED_{50} based on this available information, since it hypothesized that water in skin is the primary energy absorber and the water absorption coefficient changes significantly between 1.5 and 10.6-microns. The water absorption coefficient is 1.09×10 cm^{-1} at 1.5-microns, 1.22×10^2 cm at 3.8-microns, and 8.69×10^2 cm at 10.6-microns (Hale and Queery).

Cornea vs. Skin Anatomy

The anatomy of the cornea is different from the anatomy of skin. The cornea is made up of five layers, as demonstrated by Snell and Lembert, and is listed below from front to back:

1. The corneal epithelium (50 to 60 microns thick) has no melanin,
2. Bowman's membrane (8 to 12 microns thick) acellular collagen,
3. The substantia propria 90% of the cornea, made of four types of collagen,
4. Descemet's membrane (10 microns thick) basement membrane of the endothelium

5. The corneal endothelium (single layer of cells) actively transports fluid to the cornea

Skin epidermis can range from 500 microns thick as seen in the eyelid up to 1500 microns thick as seen in the palms and soles of the feet. It has five discrete layers from the bottom and moving outward (McKee):

1. The stratum basale anchors the epidermis firmly but, not rigidly to the dermis. This layer also produces the cells that make up the stratum spinosum.
2. The stratum spinosum begins production of keratin.
3. The stratum granulosum, continues to produce keratin, allowing for rapidly dividing cells called keratinocytes
4. The stratum lucidum, present only in very thick skin.
5. The stratum corneum, protective outer layer

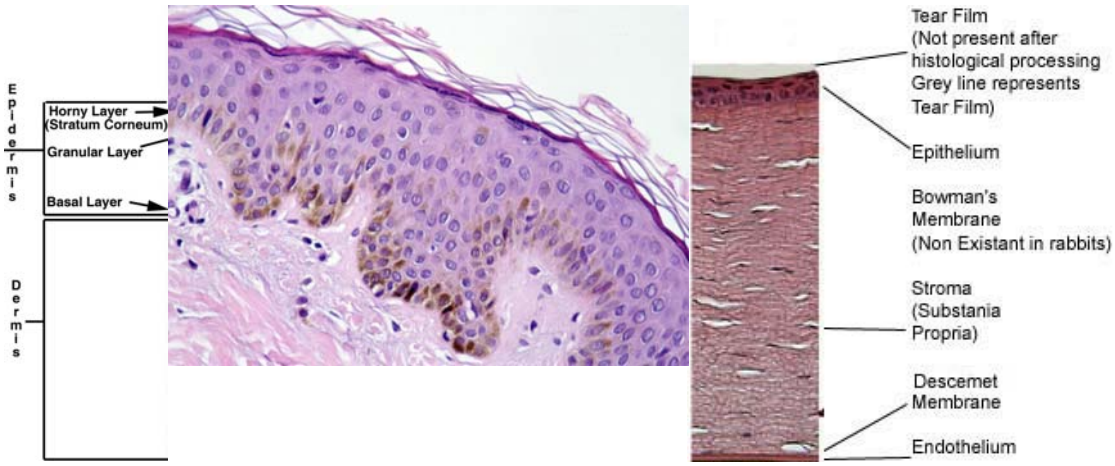

Fig. 1 Anatomy of human skin vs. rabbit cornea

CHAPTER THREE: MATERIALS AND METHODS

Introduction

The goal of this study is to determine the dose response relationship for both gross and histologic skin changes to both human engineered skin equivalents and porcine skin. This data can be used to verify the safety standards that are in currently in place.

In-vitro models, engineered human skin

Stock cultures of low passage (<6 replication cycles) human keratinocytes and human dermal fibroblasts were used as seed cultures for the production of 18 engineered human skin equivalents. Skin equivalents were circular in design and 12 mm in diameter. Set #1 was composed of six equivalents which were exposed with a laser spot size of 1 cm^2 and were used to establish initial laser parameters. Set #2 consisted of 12 equivalents which were exposed to a laser spot size of 5 cm^2 used to characterize laser-tissue interactions. All keratinocyte cultures were grown in F12/DMEM media (MediaTech) supplemented with 10% NuSerum (Collaborative Biomedical), 2 mM L-glutamine, 100 IU/ml penicillin, 100 µg/ml streptomycin and 0.25 µg/ml amphotericin. All dermal fibroblast cultures were grown in DMEM media (MediaTech) supplemented with 10% NuSerum (Collaborative Biomedical), 2 mM L-glutamine, 100 IU/ml penicillin, 100 µg/ml streptomycin and 0.25 µg/ml amphotericin. Skin equivalents were produced in two steps. First, a liquid collagen/dermal fibroblast seed culture suspension was added to a Transwell (Costar, Corning Life Sciences, Kennebunk, Maine) polycarbonate tissue culture insert contained within a 12 well tissue culture plate. Type I collagen (BD

Biosciences Discovery Labware, Bedford, Massachusetts) was used in all cases. The polycarbonate membrane of the insert served as a platform for the gelatinization of the collagen and the growth of dermal fibroblasts. Second, a cell suspension of keratinocytes was plated upon the collagen/fibroblast gel and grown in culture for 4 weeks.

In-vivo models, Yorkshire pigs

All procedures were carried out in accordance with the Guide for the Care and Use of Laboratory Animals under a protocol approved by Uniformed Services University of the Health Sciences (USUHS), Institutional Animal Care and Use Committee (IACUC). Animal housing was in accordance with requirements of the Council on Accreditation for Assessment and Accreditation of Laboratory Animal Care (AAALAC International). Five Yorkshire pigs were obtained from Archer Farms, Darlington, Maryland and maintained under anesthesia using isoflurane gas (Abbott Laboratories, North Chicago, IL) set at an infusion rate of 1 - 1.5% with oxygen flow at 22.0ml/kg/min (10.0ml/lb/min) for all exposures. Analgesia was administered (Buprenorphine 0.005 to 0.01 mg/kg IM) prior to recovery, post recovery and as needed upon evaluation every 8-12 hours. The animals were positioned based on skin exposure location (flank.) The hair was clipped, rather than shaved, on both flanks prior to exposure. Anesthesia was monitored in the pigs using toe-pinch response. Important test animal physiologic parameters such as tissue oxygenation status and core body temperature were monitored using a reflectance pulse oximeter (Vet Ox SDI 4402, Heska Corp., Ft. Colins, Co) and temperature monitor (Temp Plus 2080, IVAC Crop., San Diego), respectively. Animals were kept warm throughout the experimental procedures with a heated blanket. Thirty-four representative

6-mm biopsies were taken immediately after exposure and again at one hour following exposure while the animals were still under anesthesia. Three of the biopsies were frozen and 31 of the biopsies were preserved in formalin for histologic analysis. Sutures were placed and topical antibiotics were administered at each biopsy site. The animals were re-examined 24-hours post laser exposure for evaluation of lesion progression periodically for six days post-exposure. The pigs were anesthetized and representative laser exposed areas were biopsied for histopathological evaluation the day each pig was initially exposed, 24-hours post-exposure and 48-hours post-exposure. After completion of the observation period, all animals were transferred for use in other protocols.

Laser exposure parameters

A deuterium fluoride laser was utilized for all exposures. The laser produced a single 4-microsecond pulses at 3.8-microns. A square focal spot was used for exposures and was approximately 4 cm^2 in area. The exact spot size was calculated immediately prior to exposures and verified post exposure. Beam energy and pulse duration were sampled and verified for each exposure. Exposures ranged from 8.2 J/cm^2 to 90.7 J/cm^2 for 16 *in-vitro* exposures, (plus two unexposed control samples) and 0.01 J/cm^2 and 86.6 J/cm^2 for 56 *in-vivo* exposures.

Post-exposure tissue processing

All 18 post-exposure human skin equivalents and three porcine skin biopsies were frozen in cryosection embedding media on site using a chilled hexane bath surrounded by

liquid nitrogen. Frozen tissue sections measuring six-microns in thickness were prepared for all 21 specimens and stained using a standard Hematoxylin and Eosin (H&E) method. Thirty-one porcine tissue samples were preserved in formalin. Interpretation of laser-tissue interactions were made using subjective histopathological criteria. To best characterize the findings, a range of energies was used for the laser exposures, as well as visual, microscopic, and histologic diagnostics. Three graders visually analyzed the exposure sites as described by Rico (Rico et al). The histologic samples were examined for depth of morphologic change by using a Leica DMLB microscope, (Leica Microsystems AG, Wetzlar, Germany**)** that utilized Q-Imaging micropublisher and Q-Capture software **(**Burnaby, B.C. Canada**)**.

Response Examined	**Fluence**	**#Slides**
Mild:	**6.7 J/cm^2**	**2**
	9.5 J/cm^2	**1**
	10.0 J/cm^2	**1**
	10.3 J/cm^2	**3**
	12.6 J/cm^2	**3**
	12.9 J/cm^2	**3**
		Total 13
Moderate:	**16.4 J/cm^2**	**1**
	17.8 J/cm^2	**3**
	21.6 J/cm^2	**1**
	26.4 J/cm^2	**3**
	28.5 J/cm^2	**2**
	35.8 J/cm^2	**1**
	38.2 J/cm^2	**1**
		Total 12
Marked:	**39.4 J/cm^2**	**3**
	52.3 J/cm^2	**1**
	73.4 J/cm^2	**3**
		Total 10

Table 2. Summary of acute *in-vivo* biopsies

Statistics

All lesion grades were entered into a Probit statistical analysis package to determine the statistical threshold for gross skin morphological changes (Easy Probit version 1.0 1998). The threshold technique as described by McCally was also utilized for additional analysis (McCally and Bargeron).

Calculation of ED_{50}: Probit Anaylsis

Probit analysis is a method to statistically evaluate discrete, research data. Each exposure site or data point is evaluated by three graders as a yes, "1" or a no, "0", depending upon whether or not a particular skin change is observed. The corresponding fluence level, (J/cm^2), of the data point and its corresponding classification is utilized to ascertain the ED_{50}. Probit creates a probability curve for the reaction under consideration. Fiducial limits of 95% were used for this study. The 50% probability, (ED_{50}), of observing a specific skin change at a particular fluence level was then estimated (Finney).

Calculation of ED_{50}: Threshold Technique

The threshold technique is used to determine damage thresholds for data with little to no overlap. The threshold technique only applies when an observed reaction is clearly defined. Progressing from lowest to highest fluence possible, each exposure's fluence level and classification of observed change is documented. The fluence levels of each

exposure site serve as a data point above and below the thresholds for its corresponding, observable skin change (Bargeron et al. 1980; McCally and Bargeron 2001). For each level of skin change the range between these two points is then narrowed until there is a 10% difference, (±5%). The threshold center is the midpoint of this range.

Determination of Damage Scale

Based on the observed tissue responses, a three-tiered subjective gross skin damage scale was derived (i.e. mild, moderate and marked) in which all graders were in agreement for every exposure categorization. The damage scale is detailed in Figures 2 to 19. The severity of the elicited responses was directly proportional to increasing fluence.

Determination of Average Depth of Energy Penetration

Histologic sections were examined using a Leica DMLB microscope. An average of four sequential snapshots of the area of interest were taken at each exposure site using Q-Capture software. The file was saved with its corresponding magnification, zoom and fluence level information. Image-Pro Discovery software was used to measure the image for depth of energy penetration. First, an appropriate scale was calibrated for the level of magnification for the specific snapshot. Next, two parallel lines were manually traced: one outlining the solid portion of the stratum corneum across the length of the exposure site and a second line outlining the extreme lower edge of the damaged area across the length of the exposure site. Because the damage was at variable depths it was then

necessary to draw an average of 25 vertical lines for connecting the two parallel outlines for each snapshot. Using the average depth of energy penetration for each snapshot, the overall average depth of energy penetration was calculated for that specific exposure site, at that specific fluence.

CHAPTER FOUR: RESULTS AND DATA ANALYSIS

In-vitro models, engineered human skin

The engineered human skin samples elicited responses that ranged from mild to marked alterations of the epidermal and dermal layers within the fluences of 8.2 to 90.7 J/cm^2, used for the exposures. That damage scale is detailed in figures 2-8.

Gross changes were not detectable in the *in-vitro* models at low fluences (8.2 J/cm^2 and less). The principal histologic finding associated with the mild response was limited ablation of the most superficial layer, the stratum corneum (Fig. 2). The stratum corneum was lifted from the underlying epithelial cell layers at fluences of 11.6 to 17.8 J/cm^2 (Fig. 4). The boundary between the stratum basale and the dermis, as well as the dermis itself was as it was seen in the control (Fig. 3).

The second tier in the subjective evaluation was the moderate response, 17.8 to 54.6 J/cm^2; characterized by more prominent damage to the epidermis and a horizontal cleavage plane in the mid-epidermis (Figs. 5 and 6). Gross examination revealed alteration and slight discoloration on the tissue edge. The histopathology showed that the stratum corneum and the upper half of the stratum spinosum were absent from the exposure site (Fig. 6). There was also moderate separation between the basal layer from the underlying connective tissue, which appeared unaffected (Fig. 6).

The third tier in the subjective evaluation was the marked response, 54.6 to 90.7 J/cm^2. Histologic features of the marked response included a markedly altered epidermis with prominent clefts in the tissue. The asterisks in figure 7 indicate a grossly observable

fissure in the tissue, that was related to epidermal clefts seen in histology. The histopathology at this fluence revealed epithelial damage consistent with thermally-induced, coagulative necrosis. Several areas of the epithelium appeared to be completely removed from the underlying connective tissue (Fig. 8). At the highest fluence levels the epithelium was again separated from the underlying connective tissue and its upper edge appeared splintered. The dermis also showed areas of collagen alteration indicated by a different staining reaction than similar tissues (Fig. 9).

1. Mild response without cleavage of epithelial layers - characterized by limited damage to surface epithelial cells (stratum corneum): 11.6 J/cm^2

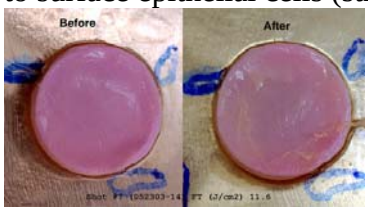

Fig. 2. *In-vitro* engineered human skin at 11.6 J/cm^2

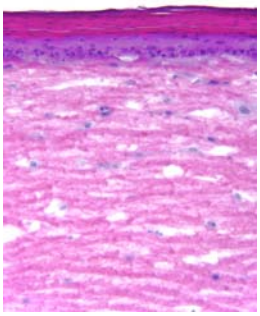

Fig. 3. *In-vitro* engineered human skin at 11.9 J/cm^2

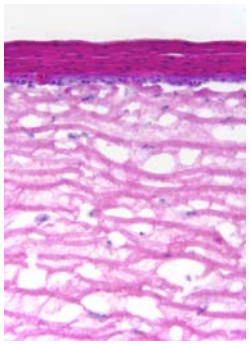

Fig. 4. *In-vitro* engineered human skin control

2. Moderate response with cleavage of epithelial layers – characterized by tissue separation along a mid-epithelial plane: 17.8 J/cm^2

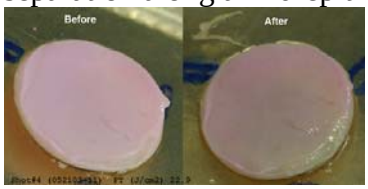

Fig. 5. *In-vitro* engineered human skin at 22.9 J/cm^2

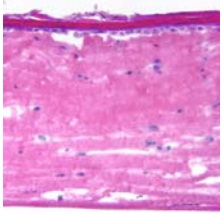

Fig. 6. *In-vitro* engineered human skin at 17.8 J/cm^2

3. Marked response – characterized by significant damage to surface epithelial cells: 54.6 J/cm^2

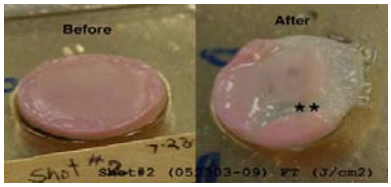

Fig. 7. *In-vitro* engineered engineered human skin at 54.6 J/cm^2
**Indicates a cleft in the tissue

Fig. 8. *In-vitro* engineered human skin at 55.0 J/cm^2

Fig. 9. *In-vitro* human skin at 90.7 J/cm^2

In-vivo porcine skin model: Immediately post-exposure

There were four levels of porcine skin responses: skin erythema, mild, moderate and marked alterations of the epidermal layers within the range of fluences used for the 55 exposures, (0.01 to 86.6 J/cm^2). Based on the observed porcine skin responses, a subjective visual skin damage scale was derived. The damage scale is detailed in Figures 10-20. The severity of the observed responses and their corresponding histology was directly proportional to increasing fluence.

The first observable skin change was skin erythema, characterized by reddening of the skin (Fig. 10). We were unable to analyze the observed skin reddening beyond gross observation as it was not a lasting response.

The next level of response was a mild response, grossly characterized by skin erythema and edema (Fig. 12). At low magnification (40x), the histologic appearance of

the epithelium appeared vacuolated in the superficial and mid-epithelial cell layers (Fig. 13). Higher magnification (400x) revealed epithelial damage consistent with thermally-induced, coagulative necrosis. Individual cells with expanded cytoplasmic margins and pyknotic nuclei were randomly distributed within the superficial and mid-epithelial cell layers. Histologic evidence suggests that most of the energy was absorbed in the superficial to mid-epithelial layers as the basal layer of cells appeared normal.

The gross characteristics of a moderate tissue response included increased erythema and edema when compared to a mild tissue response (Fig. 15). A histologic appearance of epithelial vacuolation was also a feature of the moderate tissue response, however, the number of cells affected were increased compared to the mild response and in some areas the epidermis had been separated from the underlying basement membrane (Fig. 16).

The marked response was grossly characterized by prominent tissue erythema and edema (Fig. 18). Histologically, the stratum corneum from tissues in this subjective group was generally thinned when compared to a mild or moderate response. A histologic appearance of epithelial vacuolation was also a feature of the marked tissue response, however, a more generalized effect was noted when compared to a mild or moderate responses (Fig. 20). The stratum corneum and the stratum granulosum had less pronounced damage than the deeper epithelial cell layers. Vacuolation occurred mainly in the layer closest to the basal layer.

1. Skin **erythema** - reddening of the skin due to dilatation of underlying blood vessels

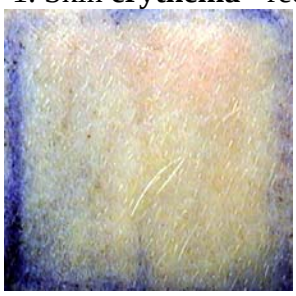

Fig. 10. *In-vivo* porcine skin at 2.6 J/cm^2

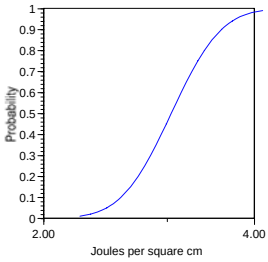

Fig. 11 Probit curve for skin erythema

2. **Mild** response – characterized by skin erythema, removal of stratum corneum.

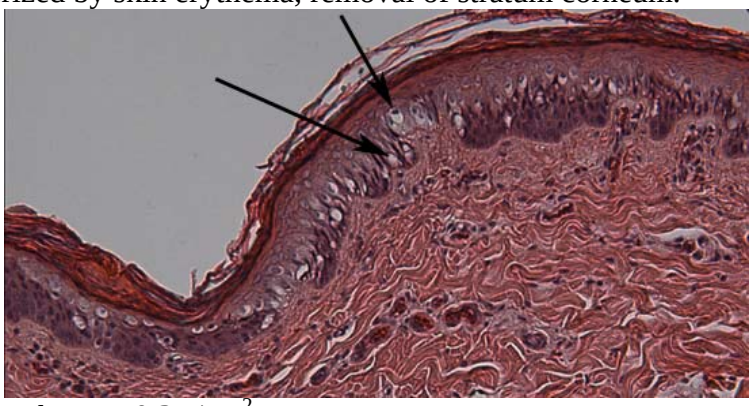

Figs. 12-13. *In-vivo* porcine skin at 10.3 J/cm^2

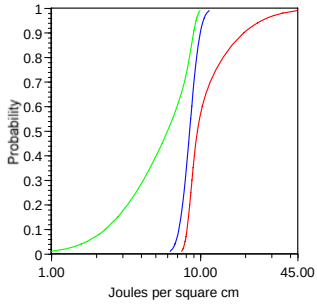

Fig. 14 Probit curve for mild skin response

3. **Moderate** response – characterized by more pronounced changes to the epithelium.

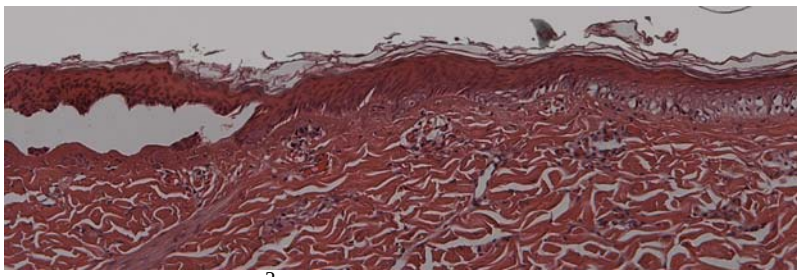

Figs. 15-16. *In-vivo* porcine skin at 26.4 J/cm^2

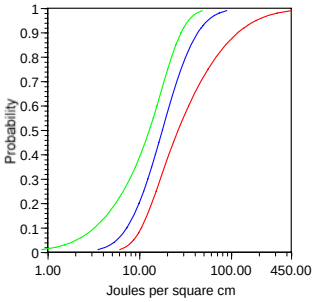

Fig. 17. Probit curve for moderate skin response

4. **Marked** response – characterized by significant changes to the epithelial layer over the entire exposure site.

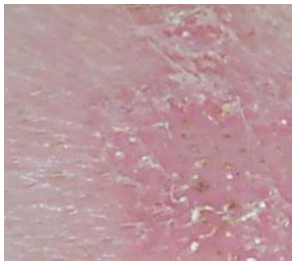

Fig. 18. *In-vivo* porcine skin at 39.4 J/cm^2

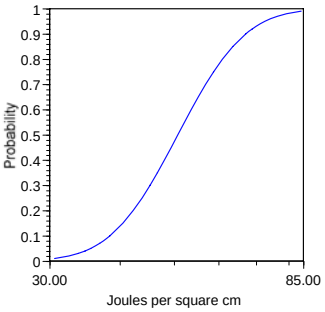

Fig. 19. Probit curve for marked skin response

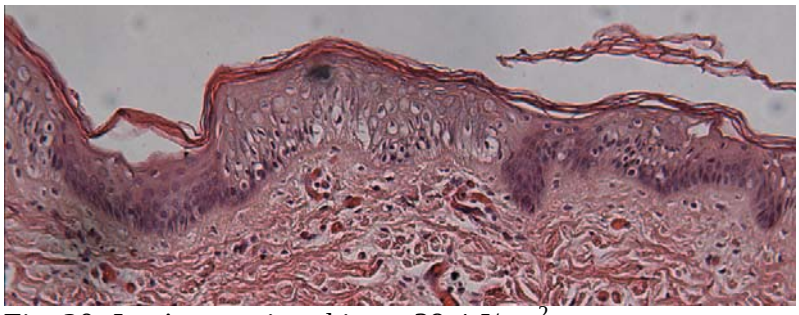

Fig. 20. *In-vivo* porcine skin at 39.4 J/cm^2

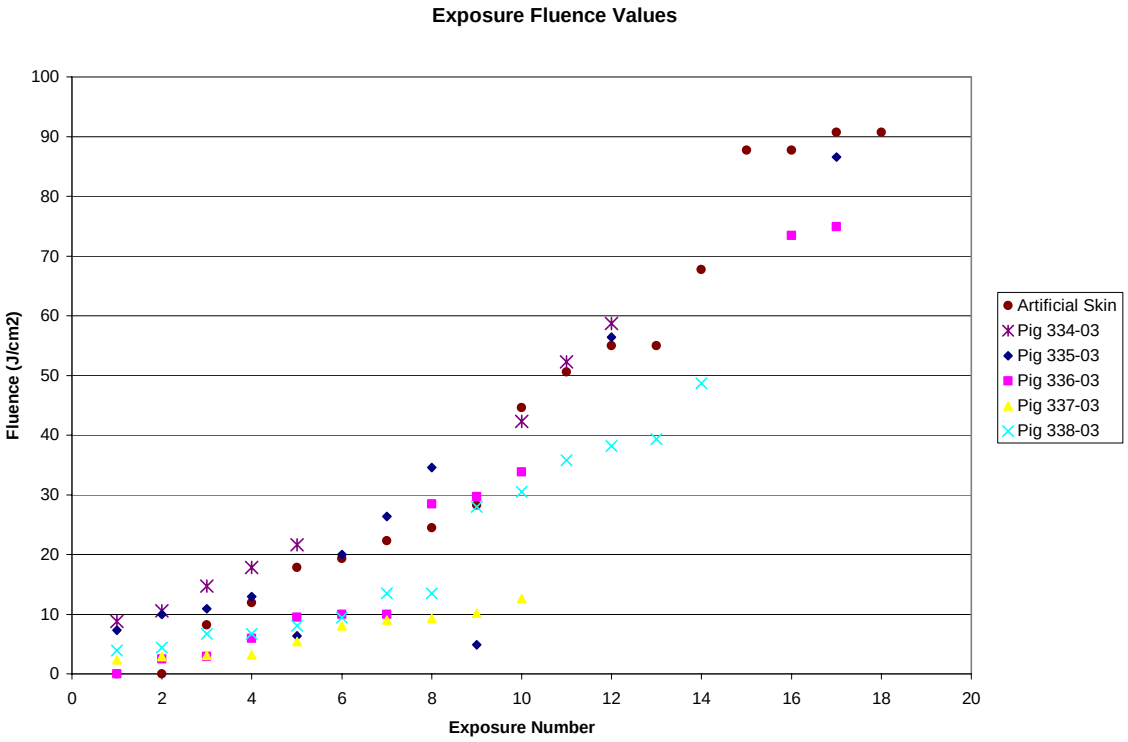

Graph 1. Fluence values for *in-vitro* and *in-vivo* exposures

Observed Response	***In-vitro*** (J/cm2)	***In-vitro*** (J/cm2)	Depth of Penetration (microns)	***In-vivo*** (J/cm2)	***In-vivo*** (J/cm2)	Depth of Penetration (microns)
	Probit	Threshold		Probit	Threshold	
Erythema	Not Applicable	Not Applicable	Not Applicable	2.6 (2.5-3.2)	2.65 ± 0.29	Not Measured
Mild	Not Measured	10.05 ± 0.6	26.69	8.5 (6.3-9.57)	7.72 ± 0.81	55.9
Moderate	Not Measured	14.85 ± 0.89	28.80	18.0 (12.92-25.81)	14.1 ± 1.47	56.4
Marked	Not Measured	52.8 ± 2.2	47.99	51.0 (39.44-79.3)	50.5 ± 5.23	62.2

Table 1. Summary of results

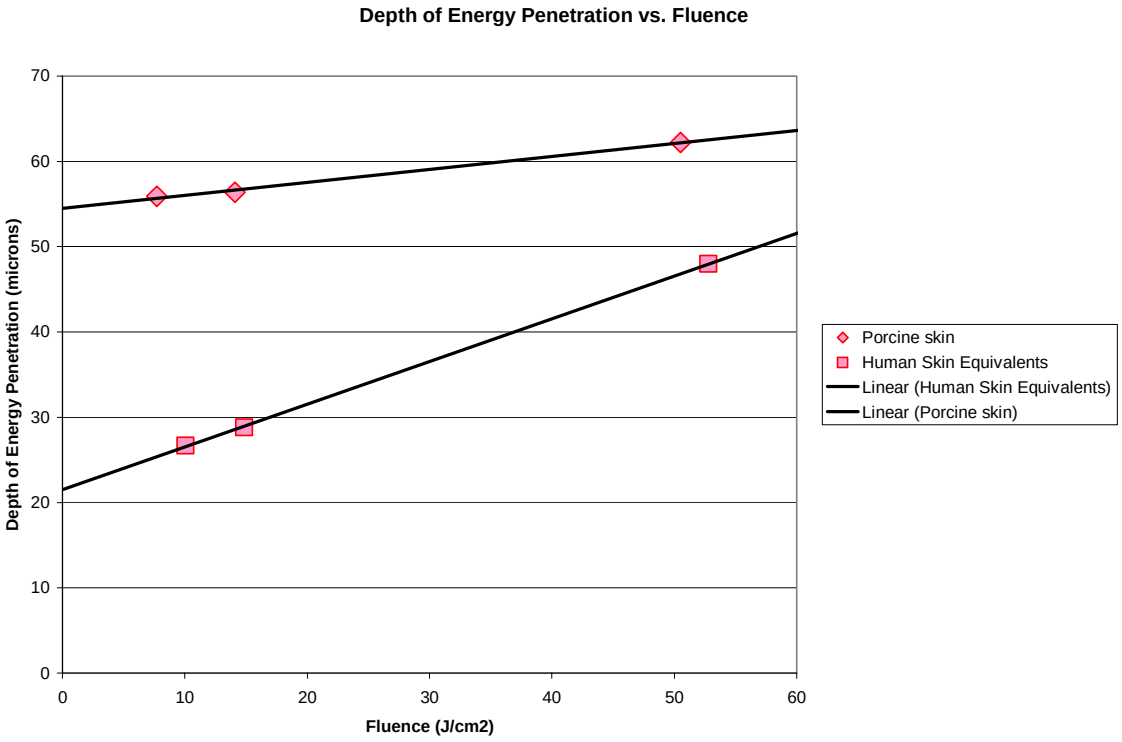

Graph 2. Depth of energy penetration compared to fluence level for *in-vitro* and *in-vivo* models

CHAPTER FIVE: DISCUSSION AND CONCLUSIONS

Discussion

In-vitro models

An important difference between engineered human skin and porcine skin is the ability of the latter to cool itself when subjected to increased heat. The vascularity of the dermis in porcine skin is the primary means of epidermal cooling (Meyer et al.). This difference may explain why the engineered human skin appeared to sustain more damage than the porcine skin following equivalent exposure conditions. It is also not yet clear if the various layers of the epidermis are more susceptible to laser energy deposition. This point may be further clarified as more data is collected on specific targets such as chromophores in the epidermal layers. Additionally, engineered human skin is not an integral part of the integument and no supporting tissues are present. This could also serve to lessen the effects present as observed with porcine skin samples.

The significant epithelial damage at 8.2 J/cm^2 in equivalents may have been from pre-exposure clefts within both the epithelium and between the stratum basale of the epithelium and the underlying connective tissue.

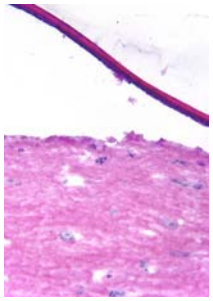

Fig. 21. *In-vitro* engineered human skin at 8.2 J/cm^2

At 44.6 J/cm^2, there was massive coagulative necrosis of the epithelium. This equivalent was part of the initial group of *in-vitro* cells, judged to be of lower quality than the second and final group, which could have been a factor in the tissue response. It may also have been due to the difference in spot size of the equivalents in set #1, (1 cm) versus those in set #2, (5 mm). One equivalent in set #2 was exposed using the same 1-cm laser spot size but the same coagulative necrosis seen in set #1 was not present. However, spot size is unlikely to be a factor. It has been shown that for spot sizes greater than 1 mm the effect of spot size is asymptotic (Cain et al.).

The depth of energy penetration differs between the human skin equivalents and the pig skin (Graph 2). One possible reason for this difference could be the presence of the pH indicator in the *in-vitro* media, which gives the equivalent their pink color. This indicator may be acting as a chromophore. Another possibility is a very specific difference between the human cell lines and the animal lines that created the dissimilarity. The method of processing the tissues may also have played a role in the deviation. There are many potential untold factors contributing to this event and further research is necessary to resolve this matter. Resolution will lead to a more efficient, robust model.

Probit analysis is a statistical method valuable in characterizing overlapping skin responses. However, in this research, we found that at low fluences, the elicited skin reaction of removal of stratum corneum and some epithelial cells had a distinct threshold and although there was some variation present in the data, there was no overlap. Probit analysis is an effective statistical method when using as few as 13 data points, but, insufficient data for each observable skin change for the human skin equivalents was

collected due to limitations in the study, (Mild: 2, Moderate: 7, Marked: 7). Consequently, the Bargeron threshold technique was used instead of Probit to better characterize the response.

The threshold technique was used to statistically describe the values for the *in-vitro* models. But, with only a total of 18 samples, or data points to work with, it was difficult to exactly pinpoint the threshold value with certainty. There were no intermediate data points between the mild response at 11.9 J/cm^2 and the moderate response at 17.8 J/cm^2. So, the resulting threshold value was an average calculation of a broad range. Also, the values listed in Table 1 reported as ± a number indicate ± a percentage value rather than a standard deviation.

At the highest fluences the histology revealed that the epidermal layer was completely lifted off the underlying connective tissue. It is hypothesized that this may be due to rapid thermal absorption of energy and subsequent expansion of tissues secondary to the conversion of water to steam.

In-vivo models: Immediately post-exposure

Some limitations in this research included the inhomogeneous profile of the laser beam that created "hotspots" across the exposure site in the *in-vivo* data. Also for *in-vitro* exposures, these "hotspots" were most likely created by the laser beam, rather than the skin surface because a consistent "H" pattern presented in all the exposure sites (Figs. 22-23). Biopsies taken on the outer edge of the exposure site made it difficult to see all of the laser-tissue interactions present across the entire tissue sample. Future research

would benefit by taking a biopsy near the center of the exposure site for comparison purposes.

Fig. 22 *In-vivo* porcine skin at 9.5 J/cm^2

Fig. 23. *In-vivo* porcine skin at 29.7 J/cm^2

Exposures less than 2.6 J/cm^2 did not produce observable changes in gross skin morphology. Analysis at the lowest fluences was limited to gross evaluation. Even so, representative biopsies taken at the lowest exposure energies in future studies would allow better evaluation of the data.

Compared to the mild response, the probability curve of the moderate response was not as steep, indicating more variability in the data. Finally, the probability curve of the marked response allowed for fiducial limits, but was steep enough to categorize epithelial cell removal over the exposure site as a possible threshold reaction.

Changes to both the gross epidermis as well as the histology to the epidermis occurred in proportion to fluence levels 0.01 to 86.6 J/cm^2. In contrast to the *in-vitro* model, the stratum corneum often remained intact. The energy appears to have been deposited mainly in the layer closest to the basal layer. It is possible that the stratum corneum and the epidermis are at least partially transparent to 3.8-micron laser light. Another possibility is that water is indeed the primary absorber, as the outer layers of skin are less hydrated. The equivalents may be more hydrated in the upper layers of the epidermis than porcine skin. Further study is necessary to ascertain the optical and

absorption properties of the stratum corneum at 3.8-microns. It is also possible that the presence of a chromophore is causing this specific pattern of deposition of energy in the porcine skin. The *in-vitro* samples may not reflect the same consistency of this chromophore; the chromophore in the *in-vitro* samples may be homogenous throughout the tissues. Whereas, the chromophore in the *in-vivo* samples is more concentrated in the epithelial layer above the basal layer. Future research should address these possibilities.

The histology of the *in-vivo* moderate response showed that the stratum corneum was partially ablated, which could be due to normal artifacts of processing, specifically normal physiologic exfoliation highlighted by the paraffin embedding and processing. When interpreting slides, it is often difficult to differentiate something of significance from normal artifacts of processing. It is possible that contributions from the laser may be hidden in the noise of processing. It is imperative to realize that the laser can exaggerate the everyday artifacts of biopsies and processing. Therefore, if the effect is not seen consistently throughout the data it must be separated from background.

Another issue in slide analysis is the potential problem of sectional geometry. The physical manipulation of taking a biopsy may change the morphology of what is seen under the microscope. Also, when the stained collagen cells of the skin naturally contract the section can fold in on itself, this is termed sectioning geometry. It is important to check and see if the stratum corneum is continuous all the way across the slice of biopsy when examined under the microscope to eliminate the possibility of this phenomenon. Some slides sectioned from the biopsies had to be re-cut to get a better view of any laser-tissue interactions. The slides utilized in this research were checked for sectioning geometry and judged to be adequate to characterize findings. Even so, it remains a

possibility in the slide analysis. Finally, the boundary effect observed in the moderate and marked responses was probably associated with a thermal disruption of the hemidesmosomes and anchoring elements of the basement membrane produced by the stratum basale.

Depth of energy penetration analysis

Examining the histology to calculate the average depth of energy penetration has limitations. The dead cells of the outermost stratum corneum are innately flaky in appearance, a fact that might even be exaggerated by the artifacts of processing. When delineating the upper edge of the stratum corneum it is necessary to use the area that is more consistent in appearance and is usually attached to the underlying layers of epithelium. Overall, one must choose the surface of the stratum corneum that is most consistent throughout the tissue section.

Preliminary analysis of photon absorption was based upon a few assumptions. We assumed that there was 100% photon absorption in the affected area with no scattering or deflectionThe energy did not appear to be deposited equally over the exposure site. Rather, the energy deposited follows a gradient. It was also assumed that the different layers of the epidermis have the same absorption properties.

Energy is not 100% absorbed in the area of interest and a percentage is actually reflected off the skin and a portion scattered. According to Takata, the percent reflected off of normal porcine skin is 3 % at a wavelength of 2.30 to 2.60 microns. Whereas, in human skin, the percent reflected is 2 % at a wavelength of 4.0 microns, regardless of

pigmentation. (Takata). The skin may also be partially shielded by momentary plasma formation during high-energy exposures.

Photons are absorbed in the layers of the porcine epidermis and it was assumed that at the lowest point of average penetration there were zero photons. It is more likely that there are a number of photons at the extreme edge of the exposure site, but not enough energy to cause any gross morphologic changes to the surrounding tissues.

Although the mild skin response had a threshold of 8.5 J/cm^2 (7.72 $J/cm^2 \pm 0.81$ using the threshold technique) and the moderate skin response had a threshold of 18 J/cm^2 (14.1 $J/cm^2 \pm 1.47$, threshold technique), the average depth of energy penetration was almost the same at 55.9 and 56.4 microns, respectively. One would expect to see a more profound dose response relationship in the average depth of energy penetration as was seen in the fluence level. Reflection and scattering of photons probably played a role in the amount of energy deposited into the tissue. Further research is necessary to better understand why there is not a more significant dose-response relationship.

Conclusions

The current skin MPE for lasers operating at the 3.8-micron wavelength for four microsecond pulses is 2.24×10^{-2} J/cm^2 (ANSI Z136. 1-2000), a value that precludes any observable skin reaction. In fact, this value is two orders of magnitude below the lowest threshold seen, (2.6 J/cm^2), for an observable skin reaction in both the *in-vitro* and *in-vivo* models. The current skin MPE may be overly restrictive, but, historical data must be taken into account when evaluating new MPE values.

Overall, both models are useful to simulate 3.8-micron laser exposures on human skin data regardless of their individual confounders. The Probit and threshold technique produce statistically identical values for each threshold reaction. Since the depth measurements vary between the models, further research is required before the use of *in-vivo* models can be fully endorsed. It would be necessary to design an experiment that can address the issue of depth of energy penetration to follow-up.

The skin of the Yorkshire pig and engineered human skin are anatomically similar to human skin. Based on the histologic review, the engineered human skin appeared to be more sensitive to gross damage than the porcine skin because the engineered human skin sustained more damage than the pig skin at comparable fluence levels. This may be a result of the capacity for epidermal cooling inherent in living tissues.

Overall, the *in-vitro* models required less complicated logistics than the *in-vivo* models. In many ways, *in-vivo* models can be difficult to utilize. It is necessary to shelter and feed the animals. In following a stringent protocol, there is no flexibility in handling or experiments conducted. More resources are required to manage and conduct the various aspects of *in-vivo* model research than are necessary for *in-vitro* models. Also, *in-vitro* models can be grown to include specific characteristics and thus, be even closer to human skin than pig skin. For such reasons, continued investigation of engineered human skin is a promising area of research.

Further analysis of this model to better characterize the method of laser tissue interaction for 3.8-micron laser-induced exposures is in progress. The role of other chromophores, including melanin in the specific observed skin reactions is an area of active investigation. Delineating laser-tissue interactions at this wavelength will prove to

be a useful baseline in future comparison studies. Also, it is imperative that more is learned about the mechanisms for these laser-tissue interactions so that appropriate safety standards can be developed.

A great deal of progress has been made in the efficacy of human skin equivalents. We are now able to meticulously grown them to meet our exact needs. In fact, current research in genomics and proteomics may someday provide new types of tests capable of replacing the *in-vivo* models. Consequently, we are at a point where *in-vitro* models are very comparable in response to 3.8-micron single laser pulses and could reasonably be expected to be used to estimate fluence required for specific tissue changes.

References

A.N. Takata, L. Zaneveld, W. Richter. 1977. Laser-Induced Thermal Damage of Skin. Technical Report, SAM-TR-77-38.

ANSI Standard Z136.1. 2000. American National Safety Standard for Safe Use of Lasers. Laser Institute of America, Inc., Orlando, FL.

B.A. Pruitt, Jr. 1997. The Evolutionary Development of Biologic Dressings and Skin Substitutes. J. Burn Care Rehabilitation, 18 (1 Pt 2): S2-5.

C. Steele. Corneal Wound Healing: A Review. 1999. Optometry Today, September.

C.B. Bargeron, O.J. Deters, R.A. Farrell and R.L. McCally. 1989. Epithelial Damage in Rabbit Corneas Exposed to CO_2 Laser Radiation. Health Physics, Vol. 56, No. 1.

C.P. Cain, G.D. Noojin. 1996. A Comparison of Various Probit Methods for Analyzing Yes/No Data on a Log Scale. United States Air Force Armstrong Laboratory, Occupational and Environmental Health Directorate, Optical Radiation Division.

C.P. Cain, T. Milner, S. Telenkov, K. Schuster, K. Stockton, D. Stolarski, B. Rockwell, W. Roach, A.J. Welch. 2004. Porcine Skin Thermal Response to Near-IR Lasers Using a Fast Infrared Camera. Proceedings of SPIE, Vol. 5319.

D.H. Sliney. 1997. Evolving Issues in Laser Safety. Journal of Laser Applications, Vol. 9(6):295-300.

D.J. Finney. 1971. Probit Analysis, third edition, Cambridge University Press.

G.C.H. Winston, T.E. Johnson, D.Q. Randolph, T.A. Neal. 2004. Evaluating acute physiological responses of porcine epidermis to a pulsed 3.8-micron laser. Proceedings of SPIE, Vol. 5312.

G.M. Hale and M. R. Queery. 1973**.** Optical Constancts of Water in the 200 nm to 200-micron Wavelength Region. Applied Optics, Vol. 12, No. 3, pp. 555-563.

G.S. Edwards, R.H. Austin, F.E. Carroll, M.L. Copeland, M.E. Couprie, W.E. Gabella, R.F., Haglund, B.A. Hooper, M.S. Hutson, E.D. Janesen, K.M. Joos, D.P. Kiehart, I. Lindau, J. Miao, H.S. Pratisto, J.H. Shen, Y. Tokutake, A.F.G. van der Meer, and A. Xie. 2003. Free-electron-based biophysical and biomedical instrumentation. Review of Scientific Instruments, Vol. 74(7) pp. 3207-3245.

I.L. Dunsky, D.E. Egbert. 1973. Corneal Damage Thresholds for Hydrogen Fluoride and Deuterium Fluoride Chemical Lasers. Technical Report, SAM-TR-73-51.

J.T. Whitton, and J. D. Everall. 1973. The thickness of the epidermis. Br. J. Dermatology, 89:467-476.

M. Ponec. 2002. Skin constructs for replacement of skin tissues for in-vitro testing. Advanced Drug Delivery Reviews, 54 Suppl. 1.

National Academy of Science (NAS) Report. 1994. Free Electron Lasers and Other Advanced Sources of Light: Scientific Research Opportunities. Commission on Physical Sciences, Mathematics and Applications.

P.H. McKee. Essential Skin Pathology. 1999. Pp. 1-2.

P.J. Rico, T.E. Johnson, M.A. Mitchell, B.H. Saladino, and W.P. Roach. 2000. Median Effective Dose Determiniation and Histologic Characterization of Porcine (Sus scrofa domestica) Dermal Lesions Induced by 1540-nm Laser Radiation Pulse. Comparative Medicine, Vol. 50, No 6, p. 633-638.

R.C. James, S.M. Roberts, P.L. Williams. 2001. General Principles of Toxicology. Principles of Toxicology: Environmental and Industrial Applications, Second Ed, p. 18-20, 561.

R.J. Rockwell Jr., L. Goldman. 1974. Research on Human Skin Laser Damage Thresholds Final Report. USAF School of Aerospace Medicine, pp. 651-652.

R.J. Rockwell Jr., W.J. Marshall, M.L. Wolbarsht, D.H. Sliney. 1992. An Overview of the Proposed Changes to the American National Standard Institute Z-136.1 for the Safe Use of Lasers. Journal of Laser Applications.

R.L. McCally and C.B. Bargeron. 2001. Epithelial Damage Thresholds for Mupltiple-Pulse Exposures to 80 ns Pulses of CO_2 Laser Radiation. Health Physics, Vol. 80, Number 1.

R.S. Snell, M.A. Lemp. 1998. Clinical Anatomy of the Eye. Second Ed. pp. 143-147.

T.A. Eggleston, W.P. Roach, M. Mitchell, K. Smith, D. Oler, T.E. Johnson. 2000. Comparison of In Vivo Skin Models for Near Infrared Laser Exposure. Comparative Medicine, Vol. 50, No. 4, p. 391-397.

T.E. Johnson, G.C.H. Winston, W.L. Greene. 2003. A Comparison of Yucatan Mini-Pig and Yorkshire Pig Skin Response to 1318-nm Laser Pulses. Laser-Tissue Interaction XIV, SPIE proceedings, Vol. 4257.

T.E. Eurell, T. Johnson, W.P. Roach. Proteomic Analyses of the Acute Tissue Response for Explant Rabbit Corneas and Engineered Corneal Tissue Models Following *in-vitro* exposure to 1540 nm Laser Light. Proceedings of SPIE, Vol., 5319.

W. Meyer, R. Schwartz and K. Neurand. 1978. The skin of domestic mammals as a model for the human skin, with special reference to the domestic pig. Current Problems in. Dermatology, 7:39-52.

W. Montagna and J. S. Yun. 1964. The skin of the domestic pig. J. Invest. Dermatology, 43:11-21.

W.P. Roach and T.E. Johnson. 2001. Porcine Dermal Lesions Produced by 1540 nm Laser Radiation Pulses. Laser-Tissue Interaction XII: Photochemical, Photothermal, and Photomechanical. SPIE proceedings, Vol. 4257.